Simulation of Dose Reduction in Digital Breast Tomosynthesis

Lucas R. Borges[1,2(✉)], Igor Guerrero[1], Predrag R. Bakic[2], Andrew D.A. Maidment[2], Homero Schiabel[1], and Marcelo A.C. Vieira[1]

[1] Department of Electrical Engineering, University of São Paulo, São Carlos, Brazil
{lucas.rodrigues.borges, igor.guerrero}@usp.br, {homero, mvieira}@sc.usp.br
[2] Department of Radiology, University of Pennsylvania, Philadelphia, USA
{Predrag.Bakic, Andrew.Maidment}@uphs.upenn.edu

Abstract. Clinical evaluation of dose reduction studies in x-ray breast imaging is problematic because it is difficult to justify imaging the same patient at a variety of radiation doses. One common alternative is to use simulation algorithms to manipulate a standard-dose exam to mimic reduced doses. Although there are several dose-reduction simulation methods for full-field digital mammography, the availability of similar methods for digital breast tomosynthesis (DBT) is limited. This work proposes a method for simulating dose reductions in DBT, based on the insertion of noise in a variance-stabilized domain. The proposed method has the advantage of performing signal-dependent noise injection without knowledge of the noiseless signal. We compared clinical low-dose DBT projections and reconstructed slices to simulated ones by means of power spectra, mean pixel values, and local standard deviations. The results of our simulations demonstrate low error (<5 %) between real and simulated images.

Keywords: Noise simulation · Dose reduction · Digital breast tomosynthesis · Anscombe transformation

1 Introduction

The ultimate study of radiation dose reduction in medical x-ray imaging requires images from the same patient at different radiation doses. In practice, such images cannot be obtained because of radiation risks. One way to overcome this limitation is to use anthropomorphic phantoms; phantom images can be acquired at various conditions without concern. However, physical phantoms do not simulate a sufficiently wide variety of breasts, which may negatively influence studies of radiologists' performance [1]. Another common approach is to manipulate standard dose images to exhibit the noise properties of an image acquired at lower radiation dose. In medical x-ray imaging, several methods have been proposed to simulate dose reduction [2–9]. However, the applicability of such methods to simulate dose reduction in digital breast tomosynthesis (DBT) is unknown.

© Springer International Publishing Switzerland 2016
A. Tingberg et al. (Eds.): IWDM 2016, LNCS 9699, pp. 343–350, 2016.
DOI: 10.1007/978-3-319-41546-8_43

Recently, we proposed a novel method of simulating dose reduction in full field digital mammography (FFDM) [9], based on noise insertion in a variance-stabilized domain, where no approximation of the noiseless signal is necessary. The method can be applied to flat fielded images. In this work, we evaluate our method to manipulate standard-dose DBT projections to mimic the noise characteristics of reduced-dose DBT projections.

2 Method

The proposed method for simulating dose reduction in DBT projections requires three sets of projection images as input: the standard-dose clinical exam and two uniform images at different doses. The two uniform images must be acquired using a uniform PMMA block, corresponding to the same kV and filtration as the clinical image. One uniform acquisition must be performed using the same exposure (mAs) as the standard-dose image; the other uniform image must be acquired using a reduced exposure time for the desired dose reduction. The three sets of images are used to generate simulated projections, which are then reconstructed to produce the reduced-dose DBT slices. Figure 1 presents the workflow used in this method.

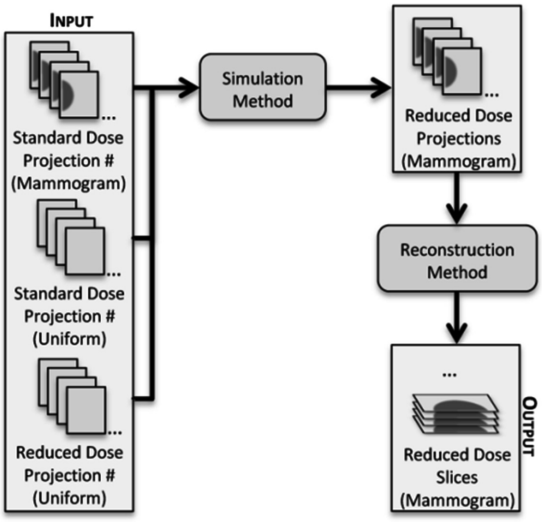

Fig. 1. Schematic of the simulation process adopted in this work.

The first stage of the simulation algorithm consists of linearizing all input images with respect to the entrance dose to the detector, and scaling the signal to the desired range. Since in this work we only consider reductions in exposure, scaling can be done simply by multiplying the original projections by the dose reduction factor (e.g., 0.7 for simulating 70 % of the dose).

The second stage of the simulation method is the noise injection. To calculate how much noise should be added to the scaled image to mimic the noise at the reduced dose, we estimate the local standard deviation on both uniform images. The difference between these estimates is then used to modulate a mask of Gaussian noise with zero mean and unity variance.

The final step is to incorporate this noise mask to the scaled image. Since the added noise must be signal-dependent, its standard deviation depends on the underlying noiseless signal. To avoid making approximations of the signal, we perform the noise insertion in a variance-stabilized domain, the Anscombe domain, where no previous knowledge of the underlying signal is necessary. Importantly, the standard deviation mask calculated previously accounts for trends in the noise statistics caused by corrections such as the flat fielding. A detailed methodology is given in [9].

3 Materials

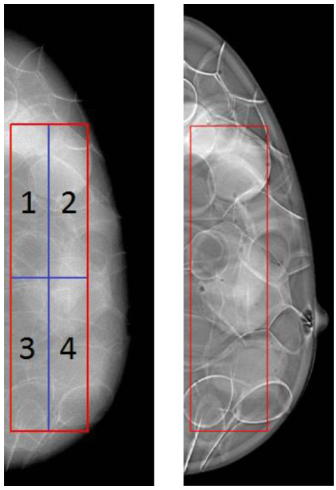

Fig. 2. Example of phantom images. Left: central raw projection. Right: central slice of the 3D reconstructed volume. The rectangles identify the ROI's used for the results. (Color figure online)

In this work we used a clinical Selenia Dimensions system (Hologic, Bedford, MA), at the Hospital of the University of Pennsylvania to assess the performance of the simulation method. Sets of DBT images were acquired using a physical anthropomorphic breast phantom, manufactured by CIRS, Inc. (Reston, VA) under license from the University of Pennsylvania [10]. The breast phantom consists of six slabs, each containing simulated anatomical structures manufactured using tissue mimicking materials, based upon a realization of the companion software phantom.

Images were acquired using a fixed tube voltage of 31 kVp, with a tungsten target, filtered with aluminum. The exposure was decreased from 60 to 30 mAs in four steps to simulate different doses. The average incident air kerma to the phantom provided by the DICOM header for each radiographic setting was: 5.62 mGy, 4.78 mGy, 3.94 mGy and 2.81 mGy. Five acquisitions were performed for each configuration, resulting in 300 phantom projections (a set of 15 projections for each acquisition). Figure 2 shows examples of a central projection before reconstruction and a central slice of the reconstructed 3D volume.

Each exposure configuration was repeated to image a uniform 4 cm thick PMMA block, commonly used for flat-field correction. Two acquisitions were performed for each exposure configuration, resulting in 120 uniform projections.

Real and simulated projections were reconstructed using the Briona reconstruction software (Real Time Tomography, Villanova, PA). Each volume was generated using 1 mm spacing, resulting in 2040 DBT slices, 1020 of them real and 1020 simulated.

To assess the simulation method we analysed images both before and after reconstruction. For the projections prior to reconstruction, three metrics were used: power spectrum (PS), local mean, and local standard deviation. The PS was calculated as the average PS of non-overlapping 64 × 64 regions within a 14.3 cm × 3.5 cm (1024 × 256 pixels) ROI containing as much breast tissue as possible, as shown by the red rectangle in Fig. 2. The spatial dependence of the PS was explored by repeating the calculations in the four non-overlapping quadrants inside the ROI, as defined by the blue lines in Fig. 2. Spatial metrics, including the mean and standard deviation were calculated inside the large ROI using 256 non-overlapping 0.45 cm × 0.45 cm (32 × 32 pixels) windows. After reconstruction of the 3D volume, we analysed mean and standard deviation of each slice, using an ROI of the same size and position as above.

The average absolute error between each simulated image and the corresponding real image was calculated for each metric at each simulated dose. The results reported are the crossed comparison between all five real and five simulated images, resulting in 25 comparisons for each metric at each dose.

4 Results

After the simulation method was applied to the DBT projections, we reconstructed the 3D volume and performed tests on both raw projections and processed slices. Figure 3 shows examples of simulated and real images.

The first metric analysed was the global PS, calculated inside the entire ROI taken from the central projection. In Fig. 4(a) it is possible to evaluate the similarity between the PS of the real and the simulated images acquired using three different doses. Figure 4(b) shows the average error between simulated and real images.

The PS was also calculated locally in four quadrants of the global ROI. This metric allows the evaluation of the spectrum of the simulated noise in different regions of the breast. Figure 4(c) shows the

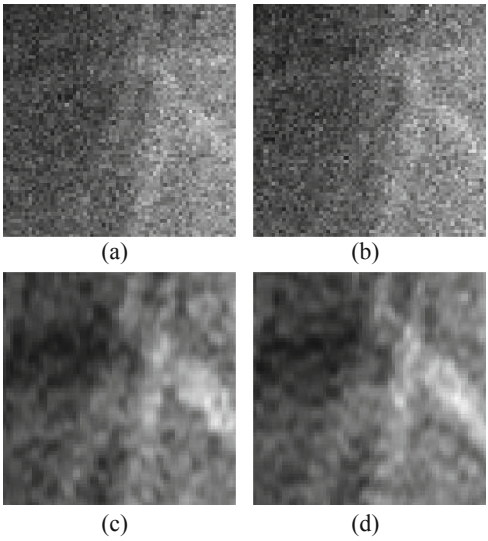

Fig. 3. Examples of real and simulated images (2.81 mGy, 50 % dose). (a) Real central projection, (b) Simulated central projection, (c) Real central slice, (d) Simulated central slice.

average absolute error at each quadrant. Note that the region used to calculate the PS on Fig. 4(c) is different in size to that used in Fig. 4(a), (b); therefore, the spectral resolution differs in the two experiments.

In the next experiment, we calculated the mean pixel value at each radiation dose and each projection before reconstruction. Figure 5(a) shows one example of the mean pixel value calculated at the central projection. Figure 5(b) is the average absolute error for each projection. Although we calculated the mean pixel value at 256 different ROIs as described in the methods section, we performed down sampling to allow better visualization of the data in Fig. 5(a); however, the errors calculated in Fig. 5(b) account for all 256 samples.

The last metric calculated on the DBT projections was the standard deviation. Similar to previous results, we give an example of the standard deviation calculated on the central slice in Fig. 6(a), and the average absolute error is reported in Fig. 6(b). Again, we performed down sampling to allow better visualization of Fig. 6(a), but the error reported in Fig. 6(b) accounts for all 256 samples.

Additional tests were performed on the reconstructed slices of the 3D volume. Figure 7(a) shows the average absolute error between the mean pixel value of the simulated and real reconstructed slices. Figure 7(b) shows the equivalent calculation for the standard deviation.

5 Discussion and Conclusions

In this work, we propose a new method for simulating dose reduction in DBT images. A number of existing dose-reduction simulation methods [2–6, 9] are based on a two-step approach: signal scaling, and noise insertion. Adding signal dependent noise to an already noisy image is a challenging task, since the noise statistics depend on the noiseless underlying signal, which is not available in most clinical cases. With the proposed method, noise insertion is performed in a variance-stabilized domain, where no knowledge of the noiseless signal is necessary. Furthermore, the method simulates noise locally; therefore, it can be applied to flat-fielded images and reproduce statistical trends, such as those generated by the heel effect.

A preliminary assessment was performed on the projection images and on the reconstructed slices. Power spectral analysis demonstrated that the noise was correctly simulated in terms of spatial frequency, with average absolute error below 3.5 % for every projection, as shown in Fig. 4(b). The average absolute error of the local power spectra reported on Fig. 4(c) shows the simulation could replicate the global and local dependencies of the clinical PS. As seen in Figs. 5 and 6, the local spatial statistics on raw projections also show small errors (<2.5 %) for every image.

The final experiment was performed on reconstructed slices. Figure 7 shows that the pixel values of the reconstruction images were very similar to the real reconstruction images, with errors below 0.5 %, and the standard deviation showed errors below 4.5 %. It is interesting to notice that in Fig. 7(a), although the errors are extremely low, it is possible to notice a trend in the results, with higher dose reductions resulting in higher errors. Furthermore, Fig. 7(b) shows that the noise was simulated

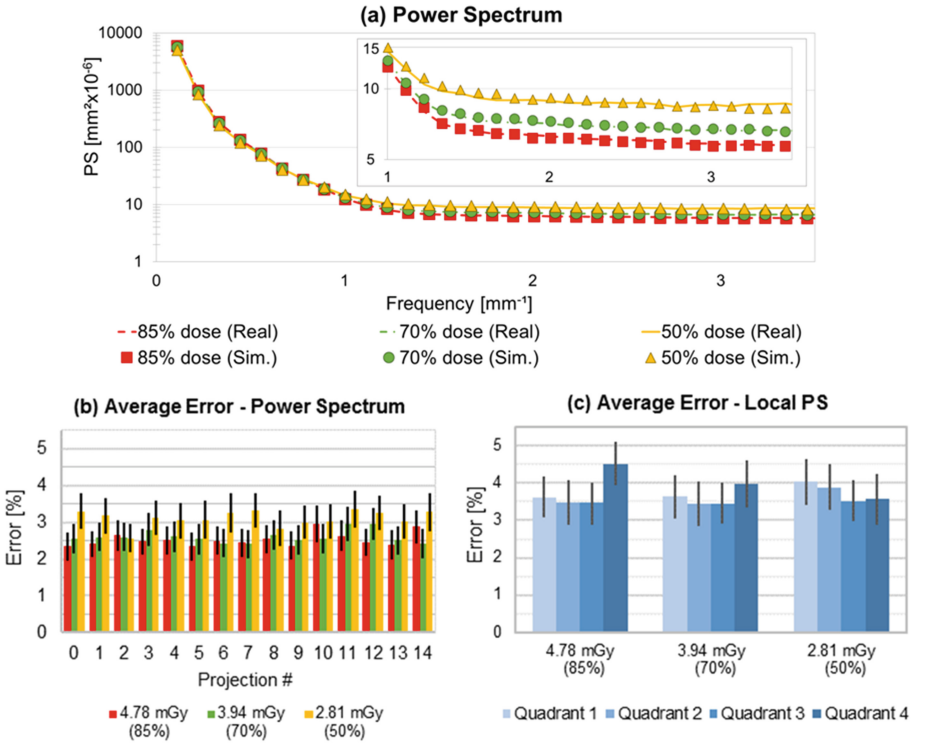

Fig. 4. Power spectra calculated from real and simulated central projections at different entrance doses to the phantom. (a) Entire spectra and high frequencies in detail, (b) average absolute error for each projection, (c) average absolute error for each quadrant. Error bars are the standard error. (Color figure online)

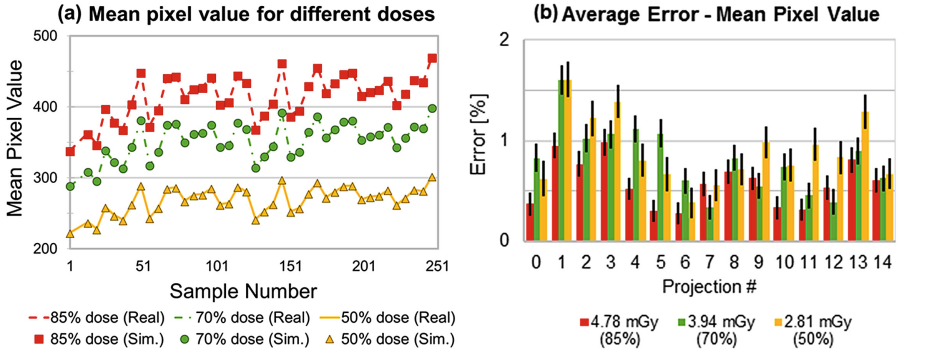

Fig. 5. Comparison between real and simulated mean pixel value at various doses to the phantom. (a) Example of the mean pixel value calculated in a central projection. (b) Average absolute error for each projection. Error bars represent the standard error. (Color figure online)

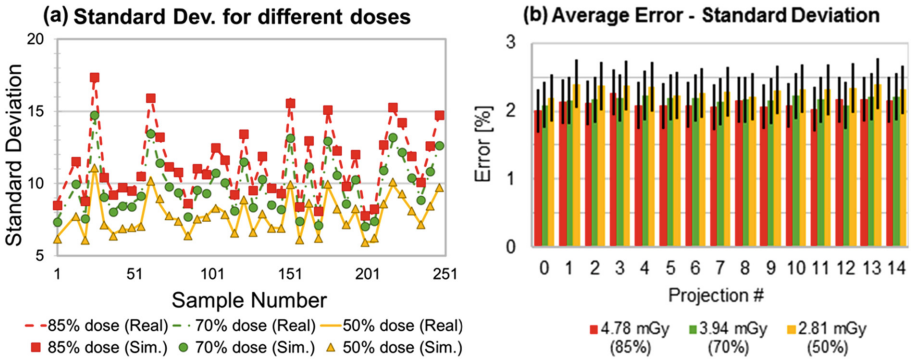

Fig. 6. Comparison between real and simulated standard deviation at various doses to the phantom. (a) Example of the standard deviation calculated in a central projection. (b) Average absolute error for each projection. Error bars represent the standard error. (Color figure online)

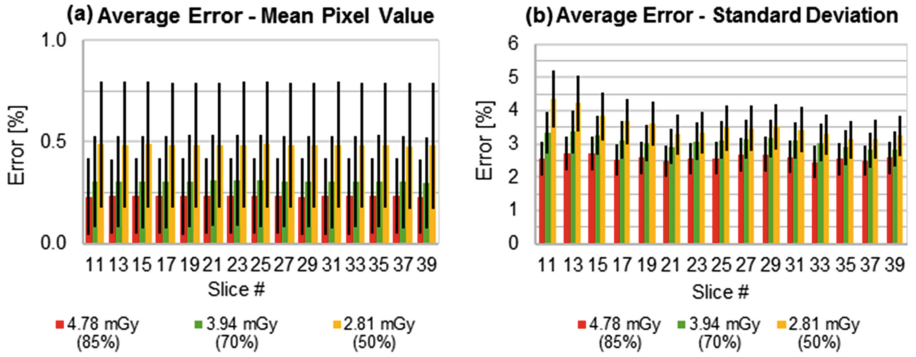

Fig. 7. Local metrics calculated from real and simulated slices at various doses to the phantom: (a) average absolute error of the mean pixel value, (b) average absolute error of the standard deviation. (Color figure online)

with higher precision in slices farther from the detector plate. Further tests are necessary to understand this behaviour.

Some limitations and future work are now addressed. In this work, we used a clinical unit with an amorphous-selenium (a-Se) detector with minimally correlated noise. Further analysis is necessary to simulate systems with highly correlated noise. In this work, we considered dose reductions achieved exclusively by reduction of the exposure. Further analysis is necessary for simulating changes on other radiographic factors, such as kV, target, and filtration. The PMMA blocks used for the uniform images were chosen to mimic the filtration of the breast. Future work should include analysis of the dependency between the thickness of the PMMA and the accuracy of the simulation method.

Acknowledgements. The authors would like to thank São Paulo Research Foundation (FAPESP grant# 2013/18915-5) and the Brazilian Foundation for the Coordination of Improvement of Higher Education Personnel (CAPES grant# 88881.030443/2013-01) for the financial support given to this project. The authors would also like to acknowledge the support of the National Institutes of Health/National Cancer Institute grant 1R01-CA154444. The content of this paper is solely the responsibility of the authors and does not necessarily represent the official views of the funding agencies. We thank Real Time Tomography (RTT) for providing assistance with image reconstruction. ADAM is a member of the scientific advisory board and shareholder of RTT.

References

1. Samei, E., Eyler, W., Baron, L.: Effects of anatomical structure on signal detection. In: Handbook of Medical Imaging, pp. 655–682 (2000)
2. Saunders, R.S., Samei, E.: A method for modifying the image quality parameters of digital radiographic images. Med. Phys. **30**, 3006–3017 (2003)
3. Båth, M., Håkansson, M., Tingberg, A., Månsson, L.G.: Method of simulating dose reduction for digital radiographic systems. Radiat. Prot. Dosimetry **114**, 253–259 (2005)
4. Kroft, L.J.M., Veldkamp, W.J.H., Mertens, B.J.A., Van Delft, J.P.A., Geleijns, J.: Detection of simulated nodules on clinical radiographs: dose reduction at digital posteroanterior chest radiography. Radiology **241**(2), 392–398 (2006)
5. Veldkamp, W.J.H., Kroft, L.J.M., Van Delft, J.P.A., Geleijns, J.: A technique for simulating the effect of dose reduction on image quality in digital chest radiography. J. Digit. Imaging **22**(2), 114–125 (2009)
6. Svalkvist, A., Båth, M.: Simulation of dose reduction in tomosynthesis. Med. Phys. **37**, 258–269 (2010)
7. Mackenzie, A., Dance, D.R., Workman, A., Yip, M., Wells, K., Young, K.C.: Conversion of mammographic images to appear with the noise and sharpness characteristics of a different detector and x-ray system. Med. Phys. **39**, 2721 (2012)
8. Mackenzie, A., Dance, D.R., Diaz, O., Young, K.C.: Image simulation and a model of noise power spectra across a range of mammographic beam qualities. Med. Phys. **41**, 121901-1–121901-14 (2014)
9. Borges, L.R., Oliveira, H.C.R., Nunes, P.F., Vieira, M.A.C.: Method for inserting noise in digital mammography to simulate reduction in radiation dose. In: Proceedings of the SPIE 9412, Medical Imaging, 94125J (2015)
10. Cockmartin, L., Bakic, P.R., Bosmans, H., Maidment, A.D., Gall, H., Zerhouni, M., Marshall, N.W.: Power spectrum analysis of an anthropomorphic breast phantom compared to patient data in 2D digital mammography and breast tomosynthesis. In: Fujita, H., Hara, T., Muramatsu, C. (eds.) IWDM 2014. LNCS, vol. 8539, pp. 423–429. Springer, Heidelberg (2014)